

MODELING SEDIMENT TRAPPING IN A VEGETATIVE FILTER ACCOUNTING FOR CONVERGING OVERLAND FLOW

M. J. Helmers, D. E. Eisenhauer, T. G. Franti, M. G. Dosskey

ABSTRACT. *Vegetative filters (VF) are used to remove sediment and other pollutants from overland flow. When modeling the hydrology of VF, it is often assumed that overland flow is planar, but our research indicates that it can be two-dimensional with converging and diverging pathways. Our hypothesis is that flow convergence will negatively influence the sediment trapping capability of VF. The objectives were to develop a two-dimensional modeling approach for estimating sediment trapping in VF and to investigate the impact of converging overland flow on sediment trapping by VF. In this study, the performance of a VF that has field-scale flow path lengths with uncontrolled flow direction was quantified using field experiments and hydrologic modeling. Simulations of water flow processes were performed using the physically based, distributed model MIKE SHE. A modeling approach that predicts sediment trapping and accounts for converging and diverging flow was developed based on the University of Kentucky sediment filtration model. The results revealed that as flow convergence increases, filter performance decreases, and the impacts are greater at higher flow rates and shorter filter lengths. Convergence that occurs in the contributing field (in-field) upstream of the buffer had a slightly greater impact than convergence that occurred in the filter (in-filter). An area-based convergence ratio was defined that relates the actual flow area in a VF to the theoretical flow area without flow convergence. When the convergence ratio was 0.70, in-filter convergence caused the sediment trapping efficiency to be reduced from 80% for the planar flow condition to 64% for the converging flow condition. When an equivalent convergence occurred in-field, the sediment trapping efficiency was reduced to 57%. Thus, not only is convergence important but the location where convergence occurs can also be important.*

Keywords. *Flow convergence, Grass filters, Hydrologic modeling, Overland flow, Sediment trapping, Two-dimensional overland flow, Vegetative filters.*

Vegetative filters (VF) are used to control sediment delivery to water bodies. VF retard flow velocity and reduce the transport capacity of water flow (Tollner et al., 1982). As a result, some of the sediment will be deposited as water flows through the VF. While there has been a significant amount of research performed on plot-scale VF and on laboratory-scale filters using either real vegetation or simulated vegetation, very little information is available on water flow and sediment transport within field-scale VF (Daniels and Gilliam, 1996; Dillaha et al., 1989, Munoz-Carpena et al., 1999; Schmitt et al., 1999; Sheridan et al., 1999). In this article, field scale differs from plot scale in that the flow lengths within the filter and the loading of water and sediment to the filter are representative of field condi-

tions, and flow pathways are not controlled by artificial plot borders.

Current models of overland flow and sediment movement through VF only apply to one-dimensional or uniformly distributed flow (i.e., planar). REMM (Lowrance et al., 2000) and VFSMOD (Munoz-Carpena et al., 1999), which are models that simulate processes that occur in VF, use this assumption. Overland flow within a VF that was investigated during this study was found to be two-dimensional with converging and diverging pathways (Helmers, 2003). Dillaha et al. (1989) stated that VF that are characterized by concentrated flow should be less effective for sediment removal than filters with shallow, uniformly distributed flow. However, there is little quantitative information on the impact of convergence of overland flow on sediment trapping in a VF. Our hypothesis is that flow convergence will negatively influence the sediment trapping capability of VF. The objectives of this investigation were: (1) to develop a modeling approach for estimating sediment trapping in a VF that accounts for converging or diverging flow, and (2) to use this model to investigate the impact of converging overland flow on sediment trapping within a VF.

MODELING

To model sediment trapping in a VF, infiltration and overland runoff must be modeled along with modeling of sediment trapping in the VF. The hydrologic processes were modeled using MIKE SHE (Refsgaard and Storm, 1995)

Article was submitted for review in March 2004; approved for publication by the Soil & Water Division of ASAE in January 2005.

A contribution of the University of Nebraska Agricultural Research Division, Lincoln, NE 68583. Journal Series No. 14506.

The authors are **Matthew Justin Helmers**, ASAE Member, Assistant Professor, Department of Agricultural and Biosystems Engineering, Iowa State University, Ames, Iowa; **Dean E. Eisenhauer**, ASAE Member, Professor, and **Thomas G. Franti**, ASAE Member, Associate Professor, Department of Biological Systems Engineering, University of Nebraska-Lincoln, Lincoln, Nebraska; and **Michael G. Dosskey**, Research Ecologist, USDA National Agroforestry Center, University of Nebraska, Lincoln, Nebraska. **Corresponding author:** M. J. Helmers, Department of Agricultural and Biosystems Engineering, Iowa State University, Ames, Iowa 50011; phone: 515-294-6717; fax: 515-294-2552; e-mail: mhelmers@iastate.edu.

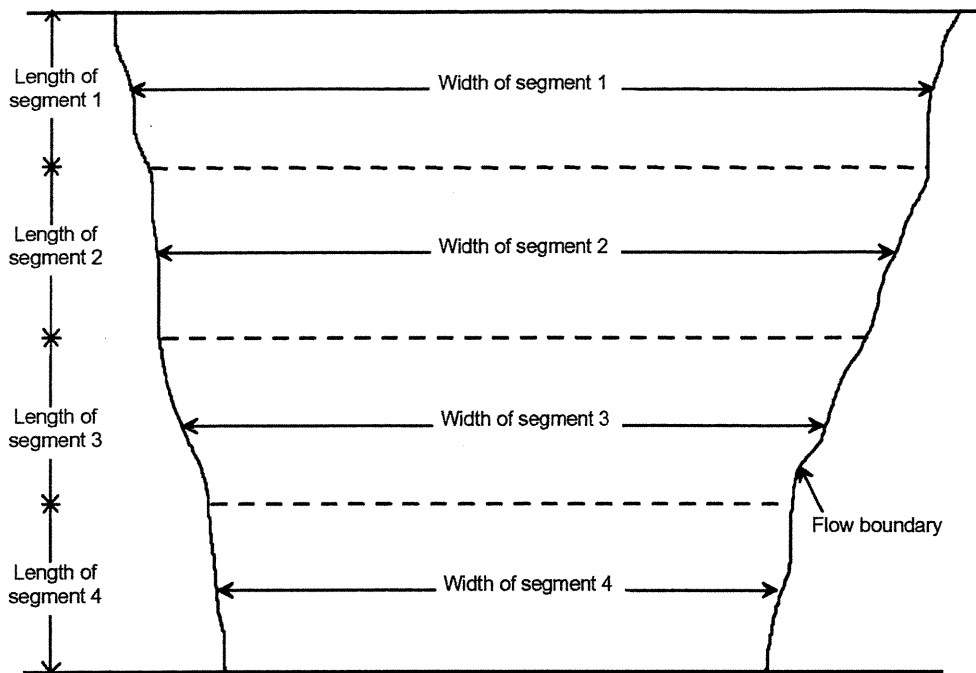


Figure 2. Segmental approach to sediment trapping in a vegetative filter. Note that segmental width varies through the filter depending on overland flow pathways, but segmental width is constant.

sediment from one segment to the next and applying the segmental trapping to determine the outflow of sediment to the next segment, the total trapping of the filter can be computed.

SEDIMENT FILTRATION MODEL

To analyze converging and diverging flow areas, the University of Kentucky sediment filtration model was programmed in a spreadsheet for use in computing sediment filtration in a VF using the segmental approach presented by Inamdar (1993). Using the segmental approach allows the width over which the overland flow is distributed to vary so that converging and diverging flow areas can be modeled (i.e., the length of each segment is constant, but the width of the segment may vary) (fig. 2). It is assumed that flow is uniformly distributed over the width of the segment. A flowchart for the spreadsheet program is provided in figure 3. The input parameters are noted in the flowchart, as are the equations used to perform the computations in each segment of the filter. To account for cases where the sediment transport capacity decreases due to diverging flow or infiltration, the sediment mass flow rate is compared to the sediment transport capacity in each segment to account for deposition by this mechanism. In the spreadsheet program, the depositional profile of the wedge is not computed, but the sediment deposition in zone D is computed to allow for use of the depth correction factor reported by Haan et al. (1994) from Wilson et al. (1982).

To compute the fraction of sediment trapped, the unit flow rate, sediment concentration, and sediment characteristics including the fraction larger than 0.037 mm must be known. The output from MIKE SHE was used in the spreadsheet model as the hydrologic input in each segment of the VF. From the coarse fraction and a particle size distribution curve, the mean particle size of the coarse fraction is computed for use in calculating the sediment transport

capacity. The mean particle size used in computation of the sediment transport capacity of the coarse fraction is the particle size at the midpoint between the fraction finer than 0.037 mm and 1. The fraction of sediment finer than 0.037 mm entering zone D is computed by:

$$D_{37} = \frac{1 - C_{f37}}{1 - f C_{f37}} \quad (1)$$

where D_{37} is the fraction of sediment finer than 0.037 mm after depositional wedge trapping, C_{f37} is the coarse fraction of sediment at the entrance to the filter, and f is the fraction of incoming coarse sediment deposited in the depositional wedge.

The average fraction finer for the coarse material is computed by:

$$D_{ACW} = \frac{1 + D_{37}}{2} \quad (2)$$

where D_{ACW} is the average fraction finer for the coarse material after wedge deposition.

The average fraction finer for the coarse material after wedge deposition is converted to the fraction finer on the original particle size distribution curve corresponding to the same particle size. The fraction finer on the original curve is computed by:

$$D_{OCW} = D_{ACW}(1 - f C_{f37}) \quad (3)$$

where D_{OCW} is the fraction finer on the original particle size distribution curve corresponding to fraction finer of coarse material after wedge deposition. The D_{OCW} value is used to estimate the mean particle size of the coarse fraction entering zone D.

compare well with the results from the example in Haan et al. (1994).

The program contains an alternative to the mixed particle size distribution by using the mean particle size (d_{50}) to characterize the sediment, as is done in VFSMOD. To further verify the model, results using this option were compared to results using VFSMOD. Two flow rate conditions were considered, both with no infiltration. The conditions considered are shown in table 1. For the $1 \text{ L m}^{-1} \text{ s}^{-1}$ peak flow rate conditions, the sediment trapping from VFSMOD was 95.1%, versus 95.9% from the spreadsheet program. For the $4 \text{ L m}^{-1} \text{ s}^{-1}$ peak flow rate condition, the sediment trapping reported by VFSMOD was 67.1%, versus 69.3% from the spreadsheet program. The results from the spreadsheet program for the mean particle size component compared well to the results from VFSMOD.

The modeling approach was applied to a specific field site, described below. The constant VF properties for this site are provided in table 2. The grass spacing is based on the average measured density of vegetation at the site. The calibrated Manning roughness coefficient is based on a tabular value from Haan et al. (1994) for a grass mixture.

Table 2. Summary of parameters in Clear Creek Buffer sediment filtration modeling.

Parameter	Value
Porosity of deposited sediment	0.50
Particle density (g cm^{-3})	2.65
Length of filter (m)	12.95
Segment length (m)	0.762
Grass spacing (m)	0.034
Slope (%), east grid	0.65
Slope (%), west grid	0.89
Calibrated Manning's roughness coefficient	0.050

STUDY SITE

SITE DESCRIPTION

Overland flow and sediment mass flow into and through a field-scale VF were monitored at the Clear Creek Buffer (see Helmers, 2003, for a detailed description of the study site and field experiments). The project site is located in Polk County in east-central Nebraska, and the VF was established in the spring of 1999. Vegetation in the filter consists of big bluestem (*Andropogon gerardii*), switchgrass (*Panicum virgatum*), and Indiangrass (*Sorghastrum nutans*). The area upstream of the VF is a furrow-irrigated field with furrow lengths of approximately 670 m and a crop row spacing of 0.762 m. The slope of the field is about 1%, and corn was grown in the field during the time period of this investigation. The field, including the filter, had been graded for furrow irrigation many years prior to this project. The furrows are perpendicular to the leading edge of the filter. The soil series in the location of the Clear Creek Buffer is a Hord silt loam (fine-silty, mixed, mesic Pachic Haplustolls) (USDA-SCS, 1974). Two $13 \times 15 \text{ m}$ grid areas in the Clear Creek Buffer were selected for investigation, with the 13 m dimension in the general direction of flow.

TOPOGRAPHY

Detailed topographic views of the two grid areas are shown in figures 4 and 5. In this research, these maps are termed the high-resolution topography. The contours on these topographic maps were developed with Surfer version 6.04 (Golden Software, 1997) using the kriging interpolation scheme. The location and elevation data (x, y, z coordinates) for these maps were obtained during the fall of 2001 using a total station (Nikon DTM-520) with measurement points on a 1.5 m grid in the $13 \times 15 \text{ m}$ area and on a 3 m grid outside the $13 \times 15 \text{ m}$ area.

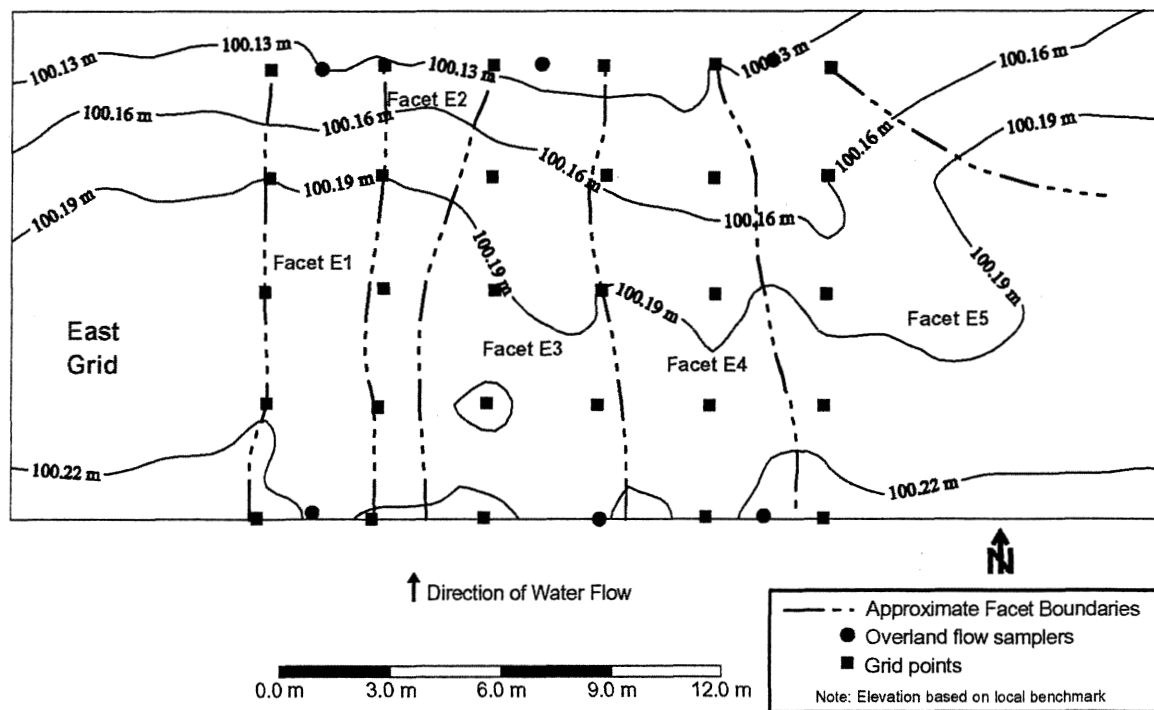


Figure 4. High-resolution topography of east grid with facet boundaries and locations of sampling equipment.

below the peak flow rate for the 1 h, 10-year return period precipitation event. The estimated volumetric inflow per unit width for a 1 h duration, 10-year return period precipitation event (11,000 L m⁻¹) was calculated using the NRCS (SCS) curve number method. This assumed a 670 m field length contributing to the filter with a SCS runoff curve number of 75 and a field slope of 1.4%. The estimated peak flow rate for this 1 h duration, 10-year return period precipitation event was calculated using HEC-HMS (USCE, 1998). The calculated peak flow rates for the precipitation event described above were approximately 2.8, 2.1, and 1.75 L m⁻¹ s⁻¹ for a 670, 400, and 300 m contributing field length, respectively. These values are greater than the average peak inflow rates, which ranged from 0.26 to 1.29 L m⁻¹ s⁻¹. In addition, using the Universal Soil Loss Equation (USLE) (Wischmeier and Smith, 1978) with a single-storm erosivity factor from Foster and Huggins (1977), an estimated erosion of 0.72 kg m⁻² was computed. This relates to an average sediment concentration of approximately 44 g L⁻¹ for the 11,000 L m⁻¹ event described above.

Using the high-resolution topography (figs. 4 and 5), the contributing area to a downstream width of 3 m was determined by drawing orthogonal lines to the contours and proceeding upstream. Orthogonal lines to the contours give approximate flow lines, and the areas between adjacent flow lines are referred to as watershed facets (Bren, 1998). Figure 4 shows the facets for the east grid, and figure 5 shows the facets for the west grid. Facets E2 and W2 have the smallest contributing upstream width of the five facets, and facets E5 and W5 have the largest upstream contributing width. The full impacts of the contributing widths of facets E5 and W5 were not reflected in the irrigation events; because the edges of the irrigation sets corresponded to the edges of each grid area, inflow did not occur along the entire contributing width. The facets provide evidence that there are likely areas of converging and diverging overland flow in the VF. Further, the facets define the converging and diverging areas that were used in modeling.

The width of the facets varied within the VF (figs. 4 and 5). Facets E3 and W3 have a greater upstream width than downstream width, and facet W1 has a smaller upstream width than downstream width. These three facets were chosen for the modeling reported in this article. Using the width of each segment and the segment discretization of 0.762 m, the area of the three facets was computed (table 4). The area of each facet was compared to the potential area of the facet without flow convergence or divergence. This ratio is referred to as the convergence ratio (CR) and is defined as follows:

$$CR = 1 - \frac{FA_A}{FA_C} \quad (4)$$

where FA_A is the actual facet area, and FA_C is the facet area assuming constant width equal to upstream facet width.

Convergence ratios greater than zero indicate flow convergence, and facets with diverging flow have convergence ratios less than zero. The convergence ratios shown in table 4 reveal that facets W1 and W3 are overall diverging facets and facet E3 is a converging facet. Only facet E3 has both an upstream width greater than the downstream width and a convergence ratio greater than zero.

Table 4. Summary of segment width for watershed facets.

Segment	Width of Facet (m)		
	W1	W3	E3
1	2.3	3.5	5.4
2	2.2	3.8	5.45
3	2.2	3.9	5.5
4	2.2	3.9	5.5
5	2.2	3.9	5.5
6	2.15	3.85	5.4
7	2.15	3.8	5.25
8	2.3	3.9	5.1
9	2.4	4	4.8
10	2.55	4	4.6
11	2.8	3.9	4
12	3.05	3.6	3.6
13	3.05	3.6	3.45
14	3	3.5	3.4
15	3	3.3	3.4
16	3	3.15	3.25
17	3	3	3
Actual facet area (m ²)	33.19	47.70	58.37
Constant width area (m ²)	29.79	45.34	69.95
Convergence ratio	-0.11	-0.05	0.17

Sediment trapping in the Clear Creek Buffer was modeled using the sediment trapping spreadsheet program. Inputs to the program included sediment, vegetation, and filter characteristics and the water flow information generated from the MIKE SHE model. For the west grid, three different conditions were simulated: planar (CR = 0), non-planar in facet W1, and non-planar in facet W3. These two non-planar condition facets were simulated because, while both facets W1 and W3 were diverging facets based on their CR values, facet W1 had an upstream width less than its downstream width, and facet W3 had an upstream width greater than its downstream width. For the east grid, two different conditions were simulated: planar and non-planar in facet E3. The non-planar condition in facet E3 was simulated because this facet represented a converging facet with an upstream width greater than its downstream width and its CR was greater than zero.

Measured and modeled sediment trapping results for the west grid events are shown in table 5. The modeled sediment trapping for facet W1 (diverging facet) is greater than either the measured trapping or the planar condition sediment trapping. The diverging facet has a greater trapping efficiency than the planar condition probably because, in general, infiltration is higher. The quantity of infiltration is reflected by the infiltration ratios shown in table 5. Infiltration increases sediment trapping, partially because of convective removal of sediment-laden water by infiltration. In addition, there is a reduction of sediment transport capacity as water is removed from overland flow by infiltration. The results for the non-planar condition for facet W3 are similar to the results for the planar conditions. Even though the ratio of upstream to downstream width of facet W3 was 1.17, the area-based convergence ratio is slightly less than zero and as a result, it is understandable that the planar and non-planar conditions are similar for facet W3. It is interesting to note the similarity between the infiltration ratios of facet W3 and those for planar flow, which is understandable since the CR for facet W3 is close to zero (CR = -0.05) so the areas for planar flow and facet W3 are similar.

Table 8. Analysis of variance for sediment trapping efficiency for east grid events.

Source	df	Pr > F
Treatment (sediment trapping computation method)	2	0.8062
Contrast		
Measured versus planar		0.58
Measured versus non-planar facet E3		0.58
Planar versus non-planar facet E3		1.0

slope of a regression line through the data was significantly different from one and to test if the intercept was significantly different from zero. From the linear regression, the slope was 1.17 and the intercept was -988 (fig. 7). Using a t-test, the intercept was not significantly different from zero at the 0.05 significance level, but the slope was significantly different from one at the 0.05 significance level. Based on the intercept not being significantly different from zero, the data were fit using linear regression holding the intercept equal to zero. For this case, the slope was computed to be 1.10, which was

found to not be significantly different from one at the 0.05 significance level. The coefficient of determination (R^2) for a 1:1 line was 0.83. Based on the slope not being significantly different from one, the measured and modeled sediment trapped compare reasonably. Considering that the modeled results are based on an uncalibrated model, the data validate the performance of the spreadsheet model for the conditions of the experiments. According to Refsgaard and Knudson (1996), validation is the process of demonstrating that a given site-specific model is capable of making accurate predictions for periods outside the calibration period. The spreadsheet model was not calibrated for the simulations that we conducted. Rather, the model's parameters were determined through field and laboratory experiments.

The greatest area-based convergence ratio for this investigation at the Clear Creek Buffer was only 0.17, but in many field conditions the ratio can be much greater. Dosskey et al. (2002) reported that the effective buffer area averaged 6%, 12%, 40%, and 80% of the gross buffer area (convergence ra-

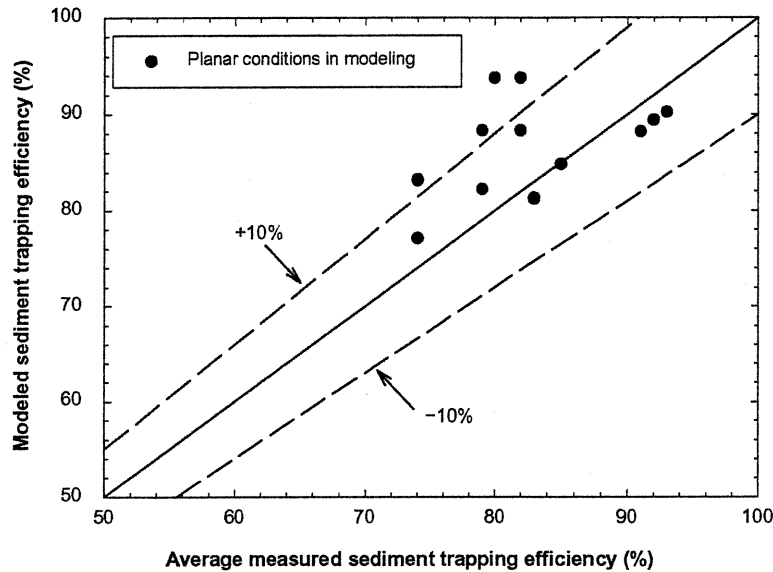


Figure 6. Measured versus modeled sediment trapping efficiency for all events.

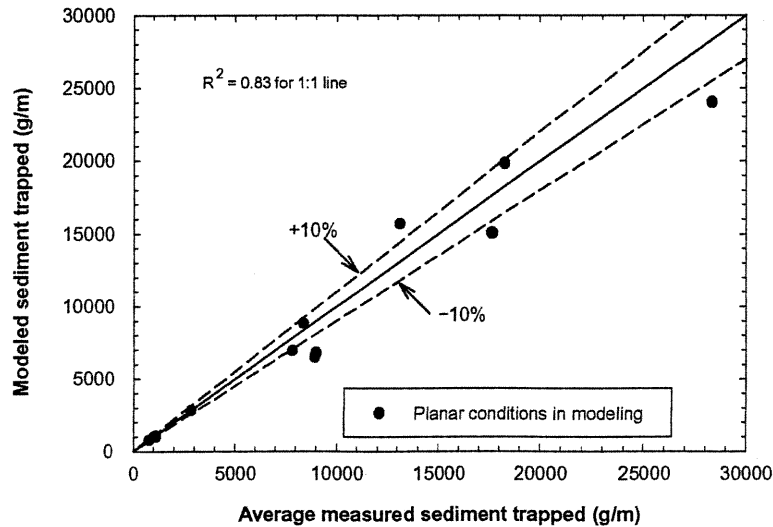


Figure 7. Measured versus modeled sediment trapped for all events.

Table 9. Combined sediment trapping efficiency for adjacent converging and diverging facets.^[a]

Flow Event	Sediment Trapping Efficiency (%)		
	Planar CR = 0	Convergence/Divergence Combination	
		CR = 0.22 and -0.17	CR = 0.31 and -0.35
Half standard flow event	87	87	87
Standard flow event (24 Aug. 2001 event)	80	78	77
Double standard flow event	64	62	61

^[a] The combined effect of having a converging facet and a diverging facet adjacent to one another.

performance. Trapping efficiency increased from 80% at CR = 0 to about 84% at CR = -0.35.

In VF where convergence occurs, there could be corresponding areas of divergence of overland flow. The inte-

grated or combined response of a converging facet next to a diverging facet was reviewed using the data from figure 8. The results for adjacent facets with convergence ratios of 0.22 and -0.17 and with convergence ratios of 0.31 and -0.35 were compared to a convergence ratio of zero (table 9). The sediment trapping efficiency is based on the overall inflow and outflow of sediment from the two facets combined. The integrated effect of these converging and diverging facets adjacent to one another had no impact at the half flow rate; when compared to planar flow (CR = 0), there was a slight reduction in sediment trapping in the filter at the standard and double flow rates.

The effect of convergence ratio at various filter lengths was also investigated using the standard runoff event. Filter lengths of 6, 9, and 13 m were used in the simulations, with a maximum convergence ratio of 0.43. As filter length decreases, the trapping efficiency decreases (fig. 9a). With no

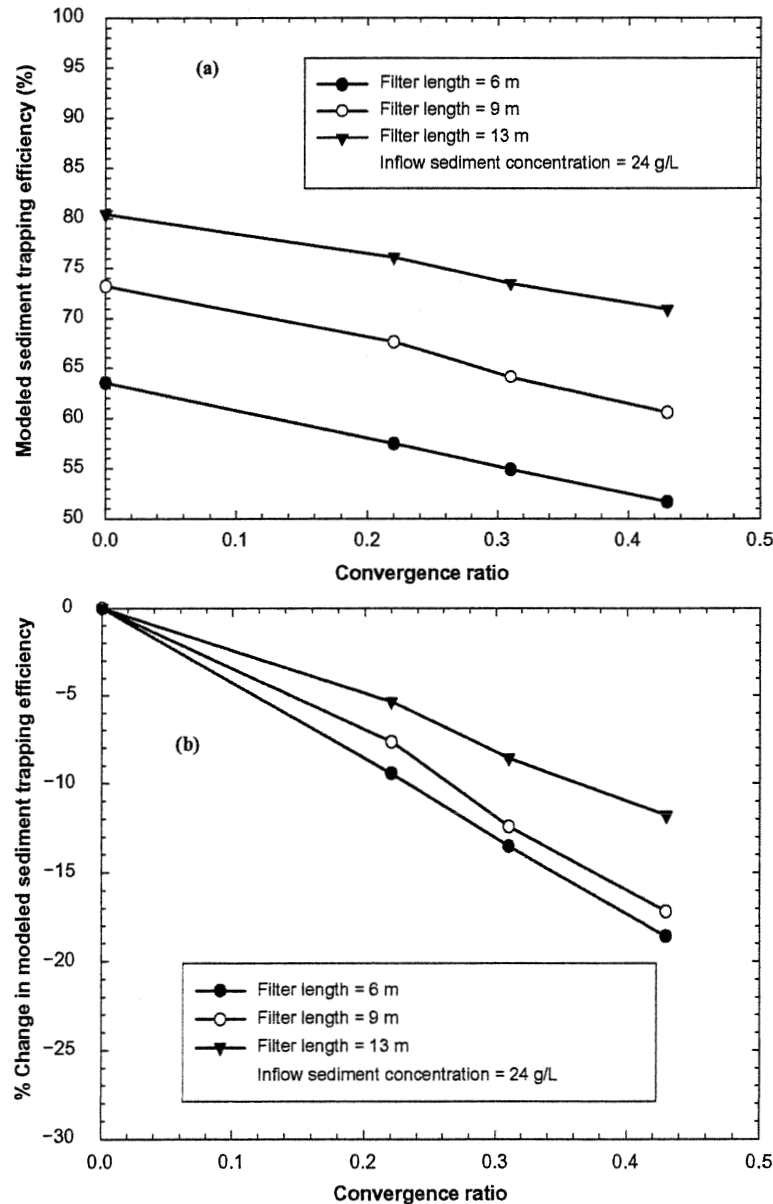


Figure 9. Sediment trapping efficiency as a function of convergence ratio for various filter lengths: (a) modeled sediment trapping efficiency, and (b) % change in modeled sediment trapping efficiency (24 August 2001 inflow rate information).

Model simulations revealed that sediment trapping efficiency is reduced as convergence increases. For example, the sediment trapping efficiency was reduced from 80% for no convergence to 62% for a convergence ratio of 0.74. The impact of convergence on sediment trapping was greater at higher flow rates and at shorter filter lengths.

The location where the flow convergence occurs is also important. Both in-filter and in-field convergence were modeled. When the in-filter convergence ratio was 0.70, the sediment trapping efficiency dropped from 80% for the planar flow condition to 64% for the converging flow condition. When an equivalent in-field convergence occurred, the sediment trapping efficiency was reduced to 57%. The combined impact of having an in-field convergence ratio of 0.5 plus an in-filter convergence ratio of 0.5 resulted in a sediment trapping efficiency of 52%, compared to 80% for the no convergence case.

ACKNOWLEDGEMENTS

The authors thank Alan L. Boldt for technical assistance and Mary Carla McCullough for management assistance during the duration of the project. Financial assistance for this project was provided in part by the Integrated Research, Education, and Extension Grants Program - Water Quality (USDA-CSREES), the USDA National Agroforestry Center, the Nebraska Corn Growers Association, and the USDA National Needs Fellowship program.

REFERENCES

- ASTM. 2000. Standard test methods for determining sediment concentration in water samples. In *Annual Book of ASTM Standards*, vol. 11.02. D3977-97. West Conshohocken, Pa.: ASTM.
- Barfield, B. J., E. W. Tollner, and J. C. Hayes. 1979. Filtration of sediment by simulated vegetation: I. Steady-state flow with homogeneous sediment. *Trans. ASAE* 22(5): 540-545.
- Bren, L. J. 1998. The geometry of a constant buffer-loading design method for humid watersheds. *Forest Ecology and Management* 110: 113-115.
- Daniels, R. B., and J. W. Gilliam. 1996. Sediment and chemical load reduction by grass and riparian filters. *SSSA J.* 60(1): 246-251.
- Dillaha, T. A., R. B. Reneau, S. Mostaghimi, and D. Lee. 1989. Vegetative filter strips for agricultural nonpoint-source pollution control. *Trans. ASAE* 32(2): 513-519.
- Dosskey, M. G., M. J. Helmers, D. E. Eisenhauer, T. G. Franti, and K. D. Hoagland. 2002. Assessment of concentrated flow through riparian buffers. *J. Soil and Water Conservation* 57(6): 336-343.
- Einstein, H. A. 1942. Formula for the transportation of bed load. *Trans. ASCE* 107: 561-577.
- Eisenhauer, D. E., M. J. Helmers, J. Brothers, M. G. Dosskey, T. G. Franti, A. Boldt, and B. Strahm. 2002. An overland flow sampler for use in vegetative filters. ASAE Meeting Paper No. 022050. St. Joseph, Mich.: ASAE.
- Foster, G. R., and L. F. Huggins. 1977. Deposition of sediment by overland flow on concave slopes. In *Soil Erosion Prediction and Control*, 167-182. Special Publication No. 21. Ankeny, Iowa: Soil Conservation Society of America.
- Golden Software. 1997. Surfer (Win 32). Version 6.04. Golden, Colo.: Golden Software, Inc.
- Haan, C. T., B. J. Barfield, and J. C. Hayes. 1994. *Design Hydrology and Sedimentology for Small Catchments*. San Diego, Cal.: Academic Press.
- Hayes, J. C., B. J. Barfield, and R. I. Barnhisel. 1979. Filtration of sediment by simulated vegetation: II. Unsteady flow with non-homogeneous sediment. *Trans. ASAE* 22(5): 1063-1067.
- Hayes, J. C., B. J. Barfield, and R. I. Barnhisel. 1984. Performance of grass filters under laboratory and field conditions. *Trans. ASAE* 27(5): 1321-1331.
- Helmers, M. J. 2003. Two-dimensional overland flow and sediment trapping in a vegetative filter. PhD diss. Lincoln, Neb.: University of Nebraska.
- Inamdar, S. P. 1993. Modeling sediment transport in riparian vegetative filter strips. MS thesis. Lexington, Ky.: University of Kentucky.
- Kutilek, M., and D. R. Nielson. 1994. *Soil Hydrology*. Cremlingen-Destedt, Germany: Catena Verlag.
- Lowrance, R., L. S. Altier, R. G. Williams, S. P. Inamdar, J. M. Sheridan, D. D. Bosch, R. K. Hubbard, and D. L. Thomas. 2000. REMM: The Riparian Ecosystem Management Model. *J. Soil and Water Cons.* 55(1): 27-34.
- Munoz-Carpena, R., J. E. Parsons, and J. W. Gilliam. 1999. Modeling hydrology and sediment transport in vegetative filter strips. *J. Hydrology* 214(1/4): 111-129.
- Refsgaard, J. C., and B. Storm. 1995. "MIKE SHE." In *Computer Models of Watershed Hydrology*, 809-846. Water Resources Publication No. 5. V. P. Singh, ed. Highlands Ranch, Colo.: Water Resources Publications.
- Refsgaard, J. C., and J. Knudson. 1996. Operational validation and intercomparison of different types of hydrological models. *Water Resources Research* 32(7): 2189-2202.
- SAS. 2002. The SAS System for Windows. Ver. 8.02. Cary, N.C.: SAS Institute, Inc.
- Schmitt, T. J., M. G. Dosskey, and K. D. Hoagland. 1999. Filter strip performance and processes for different vegetation, widths, and contaminants. *J. Environ. Quality* 28(5): 1479-1489.
- Shepherd, R. G., and W. F. Geter. 1995. Verification, calibration, validation, simulation: Protocols in groundwater and AG/NPS modeling. In *Water Quality Modeling: Proc. International Symposium*, 87-90. C. Heatwole, ed. St. Joseph, Mich.: ASAE.
- Sheridan, J. M., R. Lowrance, and D. D. Bosch. 1999. Management effects on runoff and sediment transport in riparian forest buffers. *Trans. ASAE* 42(1): 55-64.
- Tollner, E. W., B. J. Barfield, C. T. Haan, and T. Y. Kao. 1976. Suspended sediment filtration capacity of simulated vegetation. *Trans. ASAE* 19(4): 678-682.
- Tollner, E. W., B. J. Barfield, C. Vachirakornwatana, and C. T. Haan. 1977. Sediment deposition patterns in simulated grass filters. *Trans. ASAE* 20(5): 940-944.
- Tollner, E. W., B. J. Barfield, and J. C. Hayes. 1982. Sedimentology of erect vegetative filters. *J. Hydraulics Div., ASCE* 108(12): 1518-1531.
- USCE. 1998. HEC-HMS hydrologic modeling system. CPD-74. Washington, D.C.: U.S. Army Corps of Engineers.
- USDA-SCS. 1974. Soil Survey of Polk County, Nebraska. Washington D.C.: U.S. Government Printing Office.
- Wilson, B. N., B. J. Barfield, and R. C. Warner. 1982. A simulation model of the hydrology and sedimentology of surface mined lands: I. Modeling techniques. Special publication. Lexington, Ky.: University of Kentucky Department of Agricultural Engineering.
- Wischmeier, D. A., and D. D. Smith. 1978. Predicting rainfall erosion losses: A guide to conservation planning. Agriculture Handbook No. 537. Washington D.C.: USDA.

Table A.2. Nomenclature for equations A.1 through A.20.

Symbol	Definition
τ_b	The shear on the bed
ρ	Density of water
g	Acceleration of gravity
R_s	Hydraulic radius based on average spacing of media elements and the flow depth
S_c	Chanel slope
S_s	Media spacing
d_f	Depth of flow
V	Mean flow velocity
x_n	Calibrated Manning roughness coefficient
q	Volumetric water flow rate per unit width
Ψ	The shear intensity parameter
Φ_B^E	The Einstein bed load transport factor
Φ_T^E	The Einstein total sediment transport factor
ρ_s	The sediment density
d_p	Particle diameter
q_{sb}	The bed load transport rate per unit width
q_{st}	The total load transport rate per unit width
f	Fraction of the incoming coarse sediment deposited in the depositional wedge
q_{si}	Incoming sediment load rate
q_{sd}	Sediment transport rate downstream of the sediment wedge
q_{sba}	Average sediment load on the depositional wedge
T_s	Trapping efficiency in zone D(t)
q_{so}	Outgoing sediment load
R_e	Flow Reynolds number
N_f	Particle fall number
ν	Kinematic viscosity of the water-sediment mixture
V_s	Terminal settling velocity of the sediment particles
$L(t)$	Effective length of the filter
C'	Correction factor for zone D(t) trapping
T_{cs}	Corrected trapping efficiency in zone D(t)
D_{ep}	Average depth of sediment deposited in zone D(t)
I	Dimensionless term related to infiltration rate
q_{wd}	Flow rate at the inlet of zone D(t)
q_{wo}	Flow rate at the outlet of zone D(t)
f_d	Total fraction of sediment trapped in zone D(t)
T_{si}	Trapping efficiency of a segment
V_n	Mean flow velocity in segment
R_{sn}	Spacing hydraulic radius of segment
L_n	Length of segment
d_{fn}	Depth of flow in the segment
C_f	Correction factor
n	Number of segments
m	$= -0.00105(R_{et})^{0.82} (N_{ft})^{-0.91}$
R_{et}	Flow Reynolds number assuming flow properties in the segment apply to entire length of filter
N_{ft}	Particle fall number assuming flow properties in the segment apply to entire length of filter
D_{37}	Fraction of sediment finer than 0.037 mm after depositional wedge trapping
C_{f37}	Coarse fraction of sediment at entrance to filter
F	Fraction of incoming coarse sediment deposited in the depositional wedge
D_{ACW}	Average fraction finer for the coarse material after wedge deposition
$DOCW$	Fraction finer on the original particle size distribution curve corresponding to fraction finer of coarse material after wedge deposition